Received: 30 November 2021 | Revised: 20 December 2021 | Accepted: 28 December 2021

DOI: 10.1002/elsc.202100149

Engineering in Life Sciences

RESEARCH ARTICLE

A novel approach for enumeration of extracellular vesicles from crude and purified cell culture samples

Thomas Kruse | **Samuel Schneider** | **Lucas Nik Reger** | **Markus Kampmann** | **Oscar-Werner Reif**

Sartorius, Corporate Research, Göttingen, Germany

Correspondence
Thomas Kruse, Sartorius, Corporate Research, August-Spindler-Straße 11, 37079 Göttingen, Germany.
Email: Thomas.Kruse@Sartorius.com

Abstract

The interest in extracellular vesicles (EVs) has been increased in recent years due to their potential application in diagnosis and therapy of severe diseases. The versatile fields of application due to the numerous possible cargos and the targeted delivery system make them a promising biopharmaceutical product. However, their broad size range as well as varied surface protein content result in challenges for the purification, characterization, and quantification. In this study a novel method, based on high-resolution flow cytometry, was examined for the enumeration of EVs in purified as well as crude process samples. In addition to quantification, samples were characterized by dynamic light scattering, zeta potential measurement, and analytical size exclusion chromatography. It has been demonstrated that EVs were successfully enumerated with the novel method, offering great benefits for development and monitoring of EV processes.

KEYWORDS

exosome, extracellular vesicles, high-resolution flow cytometry, quantification, virus counter 3100

1 | INTRODUCTION

Extracellular vesicles (EVs) are highly heterogeneous small sized lipid bilayer enclosed vesicles, released into the extracellular space by all cell types [1,2]. These vesicles are sub-divided depending on their size, intracellular origin, and cargo [3,4]. The smallest EVs are exosomes (30–140 nm [5]), generated by inward budding of endosomes resulting in multivesicular bodies which can fuse with the plasma membrane to release the contained exosomes. In contrast, microvescicles (MVs) (100–350 nm [6]) are formed directly from the plasma membrane. A third kind of EVs are apoptotic bodies (50–2000 nm [2]) which are produced by apoptotic cells in a similar fashion as MVs.

The cargo of EVs varies depending on the condition and type of their originating cell but commonly, they carry bioactive molecules like RNA, DNA, proteins, and lipids between cells [7,8]. These transferred molecules can play an important role in cell to cell communication by mediating signals to regulate physiological as well as pathological processes [3, 9–11]. Therefore, the interest in EVs has increased in recent years due to their potential application

Abbreviations: CHO, Chinese hamster ovary; DLS, dynamic light scattering; EV, extracellular vesicle; mAb, monoclonal antibody; NTA, nanoparticle tracking analysis; PDI, polydispersity index; SEC, size-exclusion chromatography; TFF, tangential flow filtration; UF/DF concentrate, concentrated and diafiltrated clarified cell broth

as diagnostic and therapeutic tools. In particular, the utilization of EVs as drug delivery systems has gained prominence in research, mainly through their advantageous low immunogenicity, their ability to cross cellular barriers, and their potential for targeted delivery [12–14]. Furthermore, EVs and their cargo can be used as biomarkers for the non-invasive detection of several conditions like cancer, Alzheimer's disease or inflammatory diseases [15].

Due to their broad size range as well as varied surface proteins, EVs are challenging to purify, quantify and analyze [2,3]. Various EV properties can be exploited for their purification. Size-exclusion chromatography (SEC) or sequential filtration can be used to purify EVs based on size while ultracentrifugation can exploit density differences [2,16]. More recent are immunological or anion exchange chromatography purification methods which use specific surface structures or surface charge of EVs, respectively [17]. After purification, EVs have to be quantified and characterized. This can be done with bulk and single-particle analysis methods. Bulk analyses techniques for quantification of EVs, for example, proteomics, lipidomics, and western blotting, have the distinct disadvantage that they can only produce information about the average properties of the EV sample and are not able to give information about the contained EV subpopulations [18]. Due to this and the highly heterogeneous nature of EVs, single-particle analysis methods are preferred to quantify and characterize EVs [18,19].

Examples are imaging techniques like atomic force microscopy and electron microscopy. However, these techniques require extensive labeling, are limited in sample throughput and are only able to assess a small portion of the sample and are therefore low in statistical power [20–23]. Other techniques which are often used in EV research are nanoparticle tracking analysis (NTA), dynamic light scattering (DLS), and tunable resistive pulse sensing (TRPS) [15]. NTA works by measuring the Brownian motion of individual nanoparticles and uses this information to calculate the size distribution and concentration of the EVs [24–26]. However, this technique has several drawbacks for the quantification of EVs due to its low accuracy in heterogeneous samples as well as its inability to differentiate contaminants like protein aggregates from EVs [22,27,28]. Like NTA, TRPS is also used for quantification as well as size distribution analysis and additionally provides information on the charge of the measured vesicles [29].

An alternative and more specific EV enumeration method is high-resolution flow cytometry, which can detect single fluorescent molecules [30]. However, due to the small size and low refractive indices of the EVs, flow cytometers with light scattering based detector systems suffer from high background noise and are not able to reliably detect small EVs. For this reason, more sensitive methods like fluorescence based high-resolution flow cytometry are needed [31,32]. This method has recently been used for the quantification of purified EVs. Dehghani et al. were able to quantify commercially available EVs with a no-wash staining procedure with CellMask Orange (CMO) plasma membrane stain that labels the lipid membrane of EVs [33]. However, this method has not yet been investigated for enumeration of EVs from unpurified process samples, where the presence of impurities and different buffer conditions pose additional challenges to a reliable quantification method.

Therefore, in this study crude EV samples, which were produced by a Chinese hamster ovary (CHO) cell line and captured by ultrafiltration/diafiltration, were analyzed by fluorescence based high-resolution flow cytometry. To evaluate the EV enumeration capability of this method and to further characterize the EV containing samples, the size distribution and the zeta potential was assessed by DLS.

PRACTICAL APPLICATION

As for any other pharmaceutical agent, process control is crucial in order to produce future extracellular vesicle (EV) based medicine. In the case of EVs, robust enumeration methods are needed to monitor the product concentration throughout the manufacturing process. In combination with suitable fluorescent dyes, high-resolution flow cytometry has great potential in the enumeration of EVs since it can distinguish these from contaminating particles, contrary to currently available light scattering based enumeration methods. This allows the optimization and monitoring of purification steps from an early stage on and thus a more efficient EV process development.

2 | MATERIALS AND METHODS

2.1 | HEK exosomes

As a control and for the development of the EV enumeration method, purified, and lyophilized exosomes from HEK293 cell culture were purchased from HansaBioMed Life Sciences (Estonia). The lyophilized exosomes were reconstituted according to the enclosed instructions, 1:10 diluted in 1xPBS (all chemicals were purchased from Carl Roth, Germany), aliquoted and stored at −80°C until use.

2.2 | Fed-batch cultivation for EV production

One cultivation of a CHO-DG44 suspension cell line, genetically modified to express a monoclonal antibody (mAb), was used for EV production in a fed-batch process under serum free conditions. A 5 L UniVessel (Sartorius, Germany) was inoculated at 3 L with a cell density of $0.3*10^6$ cells/mL and cultivated for a total of 6 days. A proprietary CHO-DG44 basal as well as feed medium was used in a fixed bolus feeding regime.

The temperature was set to 36.8°C, the pH adjusted to 7.1 via CO_2 sparging and addition of base (1 M Na_2CO_3), DO was held at 40% by supply of O_2 to the basal gassing. The harvest was executed at day 6 as described in Section 2.3 with a viable cell density of $24.5*10^6$ cells/mL and 98.2% viability.

2.3 | Clarification and EV capture

A CHO fed-batch cultivation broth was clarified by a single-use Ksep centrifuge (Sartorius, Germany) at 1000 × *g* with subsequent sterile filtration using a 0.2 μm Sartopore 2 XLG capsule (Sartorius, Germany) to remove cell debris and large EVs. To capture the EVs (separation from low molecular weight impurities) and concentrate the clarified broth tangential flow filtration (TFF) with a Sartocon Slice 200 ECO 300 kDa Hydrosart filtration cassette (Sartorius, Germany) and a Sartoflow Smart system (Sartorius, Germany) was performed. One liter clarified broth was concentrated to 300 mL followed by constant volume diafiltration for five volume exchanges using 1xPBS (all chemicals were purchased from Carl Roth, Germany). Afterwards, a final concentration step to 45 mL was carried out by TFF, resulting in a concentration factor of 22. During all TFF steps, the inlet pressure was held constant at 1 bar resulting in a transmembrane pressure of approximately 0.5 bar. The concentrated and diafiltrated clarified broth (UF/DF concentrate) was aliquoted as product and frozen at −80°C until further use.

2.4 | EV purification with size exclusion chromatography

The UF/DF concentrate was centrifuged at 5000 × *g* for 5 min and 0.5 mL of the supernatant was loaded on a IZON qEVoriginal 35 nm SEC column (Izon Science, New Zealand) which was previously equilibrated with 1xPBS (all chemicals purchased from Carl Roth, Germany). The SEC was carried out according to the instructions provided by the manufacturer. After loading of the supernatant to the top of the column the elution was performed by adding stepwise 20 mL degassed and 0.1 μm filtered (Sartolab RF, Sartorius, Germany) 1xPBS in 0.5 mL fractions. The UV absorption at 260 and 280 nm of the UF/DF concentrate and the collected fractions was measured using an Infinite 200 Pro spectrometer (Tecan, Switzerland) and 1xPBS as blank solution.

2.5 | DLS and zeta potential measurement

DLS and zeta potential measurements were performed with a Zetasizer nano ZSP (Malvern Instruments, United Kingdom) in DTS1070 zetta cuvettes (Malvern Instruments, United Kingdom). Before measurement, samples were diluted 1:5 in reverse osmosis water and centrifuged for 5 min at 5000 × *g*. Measurements of the supernatants were taken at 25°C with a prior equilibration time of 2 min. Size measurements were always carried out before zeta potential measurements. In addition to the cumulants analysis, resulting in a Z-average (mean particle size in the sample) and a polydispersity index (PDI, measure of the heterogeneity of a sample based on size), the correlogram was also evaluated using a size distribution analysis model with 200 size classes, a lower size limit of 1 nm and an upper limit of 500 nm to calculate the size distribution by intensity. For zeta potential measurements, the unaltered general purpose analysis method of the device was used.

2.6 | EV enumeration by high-resolution flow cytometry

EV concentration determination was done using a Virus Counter high-resolution flow cytometer (VC3100, Sartorius, Germany). A half-logarithmic dilution series of the sample was executed in 1xPBS. Subsequently, the samples were stained with CMO (Thermo Fisher Scientific, United States), at a concentration of 1 μg/mL. This was done by adding 5 μL CMO staining solution with a concentration of 21 μg/mL to 100 μL diluted sample or 1xPBS for the blank sample. After incubation at room temperature in the dark for 10–60 min, stained samples were diluted 1:100 in 1xPBS and directly measured with the VC3100 with three internal replicates. The staining procedure led to a sample preparation dilution factor (SPDF) of 105. Measurements were taken at a sample flow rate of 300 nl/min and a sheath flow rate of 350 μL/min. The N channel photomultiplier tube is sensitive to CMO fluorescence and

was used with a gain setting of 0.73 V to detect the labeled particles.

Data evaluation was done by logarithmizing the dilution factor (DF) and the particle concentration measured in the N channel (C_N). Subsequently, a linear regression was carried out in the linear range of the data. The resulting slope (a) was used to calculate the undiluted concentration (C) of the diluted samples measured in the linear region according to Equation (1).

$$C = 10^{\lg(C_N) - a * lg(DF)} \quad (1)$$

Afterwards, the mean value as well as the standard deviation of the undiluted concentration in the linear region was calculated, multiplied with the SPDF and reported as the sample particle concentration ($C\mu$) and sample particle deviation ($C\sigma$).

2.7 | Determination of mAb concentration

The mAb concentration was determined by an analytical high performance liquid chromatography (HPLC) system with an SEC column [34].

3 | RESULTS AND DISCUSSION

3.1 | Feasibility of exosome enumeration and characterization

In order to establish a method for EV quantification and to verify the feasibility of enumeration of commercially available, purified EVs by fluorescence based high-resolution flow cytometry, HEK exosomes were analyzed.

The measurements demonstrated a very good linear correlation of the measured particle concentration for the dilution series, indicated by a coefficient of determination of 0.944 as well as a slope of -0.98 for the linear regression (Figure 1). To compensate for potential dilution artefacts like particle adsorption on the test tube wall, the slope of the linear regression from three internal replicates was included in the concentration calculation, instead of using the DF of the individual samples. The particle concentration of the HEK exosomes was calculated to be $7.85*10^9$ p/mL with a standard deviation of $2.55*10^9$ p/mL. This particle concentration is similar to the manufacturer's data of $1.5*10^{10}$ p/mL determined via NTA, considering that two completely different quantification methods were used and that the lyophilized HEK exosome standard had to be reconstituted and underwent one freeze-thaw cycle before measurement.

Negative controls are important to demonstrate that the measured signal used for quantification is indeed a result of present EVs. However, Dehghani et al. have already presented extensive negative controls for purified EVs of several origins quantified by the same high-resolution flow cytometer and staining dye [33]. A more than ten-fold reduction of the measured particle concentration was obtained by lysing the EVs with the detergent TritonX-100 [33]. Therefore, focus in the present study was placed on the measurement of crude samples and additional analysis methods.

For this reason, to further characterize the HEK exosomes the size distribution was investigated by DLS. Two defined peaks with different size were obtained (Figure 2A) by the size distribution analysis. The smaller fraction with a size of 83 ± 7 nm most likely represents the exosomes as it is in the range known from literature [5]. The larger fraction with approximately 400 nm probably represents some larger impurities. However, due to the underlying measurement methodology of DLS this fraction accounts for only a small proportion, since the size of the measured particles enters into the scattering intensity signal with the sixth power. The Brownian motion of particles or molecules in a suspension causes the laser light to be scattered with varying intensity. Larger particles scatter significantly more light compared to smaller ones. The analysis of these intensity fluctuations yields the speed of Brownian motion and thus the particle size using the Stokes-Einstein relationship. [35].

In addition to the size distribution, the zeta potential distribution was examined (Figure 2B). A mean value of -28 mV with a mean standard deviation of 11 mV for all measured particles was determined for the HEK exosomes. The negative charge is in good agreement with already reported measurements from the literature [36] and also demonstrates why anion exchange chromatography is often used for further purification of EVs [17]. These results confirm the suitability of DLS based measurements for exosome and EV characterization. Therefore, DLS was further used to characterize samples enumerated by fluorescence based high-resolution flow cytometry.

3.2 | Enumeration and characterization of EVs from crude process samples

The quantification and characterization of purified exosomes by fluorescence based high-resolution flow cytometry and DLS was demonstrated in Section 3.1. In the next step, crude EV containing process samples, which are especially important for the EV process development, were examined. Ultrafiltration/diafiltration, which is a commonly performed first EV capture step [37,38],

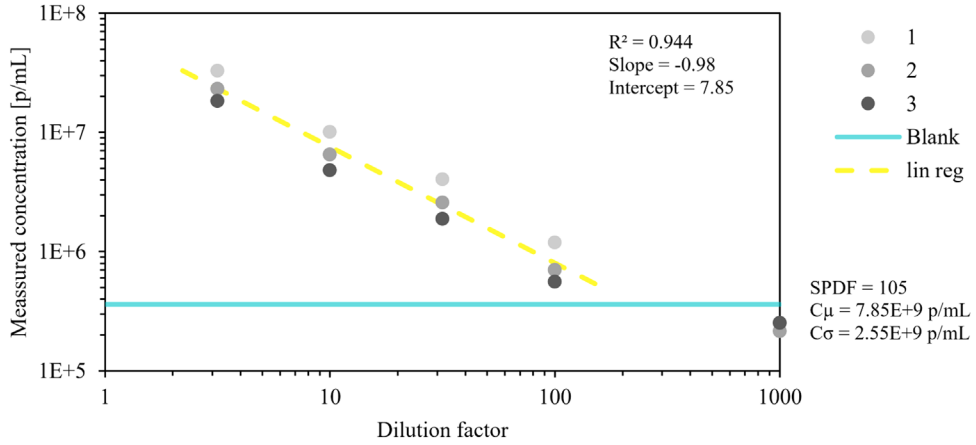

FIGURE 1 Enumeration of HEK reference exosomes. The 1, 2, and 3 labels correspond to the three internal replicates. SPDF is the sample preparation dilution factor, Cμ is the sample particle concentration of the undiluted sample while Cσ is the corresponding standard deviation. The coefficient of determination (R^2), slope of the linear regression (lin reg) and the intercept are indicated. The blue line corresponds to the average measured particle concentration of the blank sample

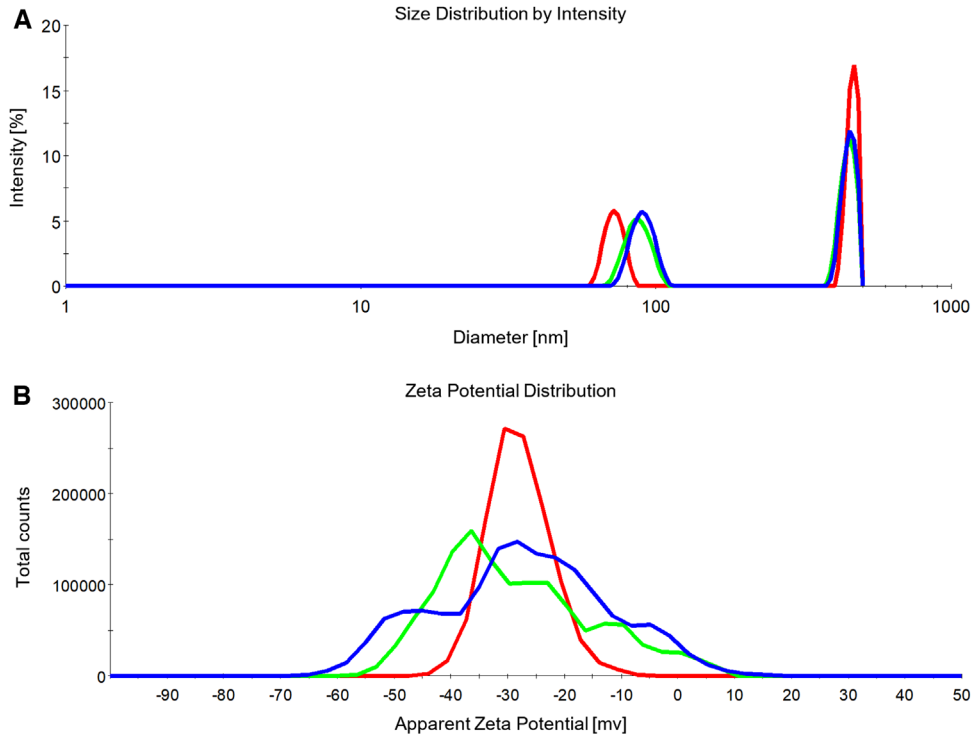

FIGURE 2 Size distribution by intensity (A) and zeta potential distribution (B) of the HEK exosomes. Analysis was performed in triplicates (red, green, and blue lines)

was performed with a clarified CHO cultivation broth to create a crude model solution. CHO cells are one of the most established cell lines in biopharmaceutical processes and naturally secrete EVs [39]. In addition, the used cell line was genetically modified to produce a mAb, which in this study represents a model for an impurity of the EV product. Crude samples contain also other process related impurities like host cell proteins and deoxyribonucleic acids as well as mAb aggregates which might have an influence on the analysis methods shown here. However, since the mAb has the highest concentration among these impurities in the sample, it was investigated more closely as a model impurity in the following.

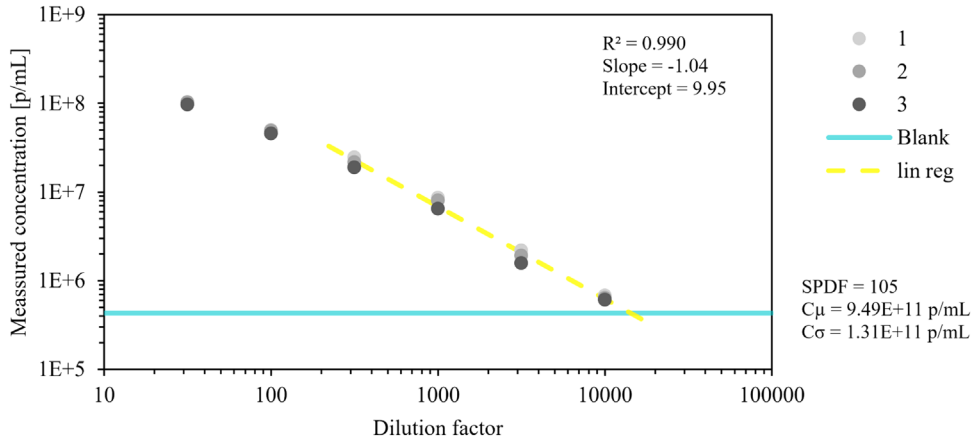

FIGURE 3 Enumeration of crude UF/DF concentrate samples. The 1, 2, and 3 labels correspond to the three internal replicates. SPDF is the sample preparation dilution factor, Cμ is the sample particle concentration of the undiluted sample while Cσ is the corresponding standard deviation. The coefficient of determination (R^2), slope of the linear regression (lin reg) and the intercept are indicated. The blue line corresponds to the average measured particle concentration of the blank sample

In order to examine the EV quantification capability of the fluorescence based high-resolution flow cytometry the crude UF/DF concentrate sample was analyzed (Figure 3).

For dilution factors between 316 and 10 000, corresponding to a particle concentration of $2.18*10^7$ and $6.42*10^5$ p/mL, a linear region with a coefficient of determination of 0.990 was obtained. The internal replicates exhibited a good reproducibility throughout all dilution factors. Based on these results, a concentration of $9.49*10^{11} \pm 1.31*10^{11}$ p/mL was calculated for the UF/DF concentrate sample. Lower dilution factors resulted in a measured particle concentration lower than the linear region, probably because the fluorescence signal of several EVs overlap at such high concentrations. Even though the particle concentration for the UF/DF concentrate sample is significantly higher than that of the HEK reference exosomes, it was possible to obtain a linear measurement range in both cases by appropriate dilutions.

For further characterization of the UF/DF concentrate the size distribution and zeta potential were subsequently examined by DLS (Figure 4A and C). Although numerous parameters must be fulfilled for the reliable classification as EV these characteristics were used as indicators.

The obtained size distribution exhibited a defined signal slightly larger than 10 nm and a broad region around approximately 100 nm. The performed triplicates exhibited a high variability, which is due to the high polydispersity of the crude sample caused by the broad particle size range. However, the majority of the intensity signal was in a range between 30 and 200 nm, which is the expected size for small EVs [5].

The size distribution signal at 10 nm was probably a result of the remaining mAb in the sample after the concentration and diafiltration process. The DLS measurements of a purified mAb sample (Figure 4B) exhibited also a defined signal at slightly above 10 nm, corresponding to the mass of the mAb (~150 kDa) [40]. Even though a membrane with a mean molecular weight cut off (MWCO) of 300 kDa was used, the UF/DF concentrate sample exhibited a mAb concentration of 6.25 g/L. This may be explained by the characteristic Y-shape of IgG which results in larger hydrodynamic diameters than it is the case in globular molecules [41] and the fact that the MWCO of a membrane represents just the average of a broad range of pore sizes [42]. In addition, fouling effects could have reduced the nominal pore size of the membrane during the ultrafiltration/diafiltration process.

The mean zeta potential of the UF/DF concentrate sample was -27 mV (Figure 4C, Table 1), which is similar to that of the commercially available HEK exosomes (Figure 2B), indicating the presence of EVs.

3.3 | SEC analysis

In order to separate the mAb as impurity from the EVs and to further characterize the crude UF/DF concentrate sample as well as the EV enumeration by fluorescence based high-resolution flow cytometry, a SEC was performed (Figure 5).

The first fractions contained the EV due to their relatively large size, resulting in an early elution from the SEC column. Accordingly, in fractions 2 to 5 high particle concentrations of up to $2.39*10^{11} \pm 4.30*10^{10}$ p/mL (fraction 3, Figure 5 and Table 1) were determined, while the later fractions resulted in a signal below the limit of detection. Fraction 2 and 3, with the highest particle concentration

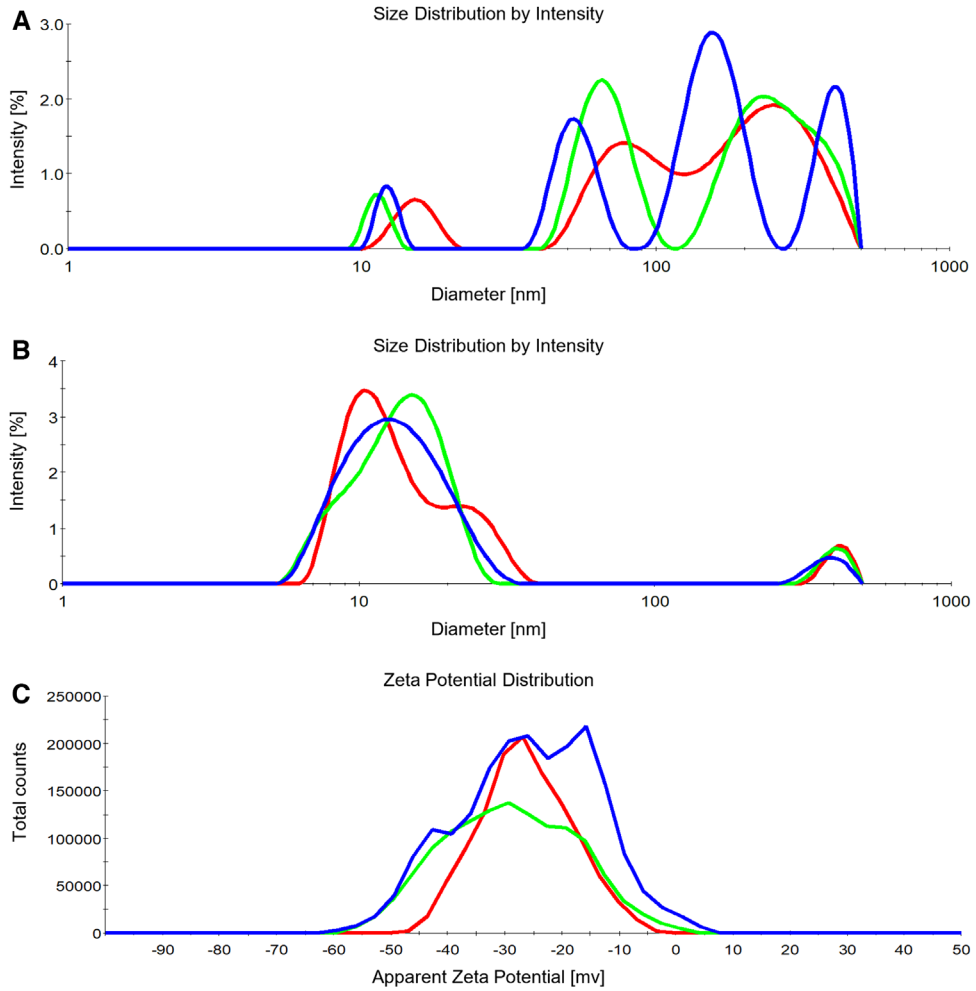

FIGURE 4 Size distribution by intensity of the UF/DF concentrate sample (A) and purified mAb (B). Zeta distribution of the UF/DF concentrate sample (C). Analysis was performed in triplicates (red, green and blue lines)

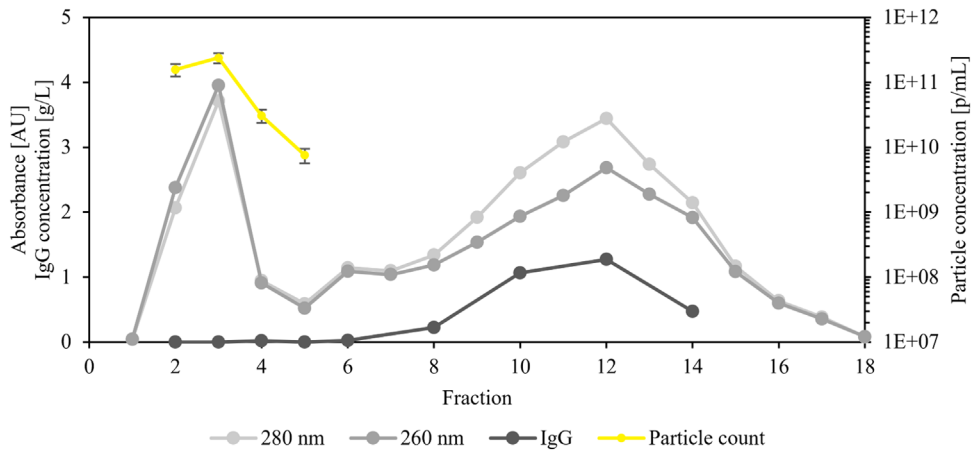

FIGURE 5 Analytical results for the SEC fractions of the crude UF/DF concentrate Sample. Error bars represent the sample particle deviation Cσ

TABLE 1 Summary of the analytical results for the EV containing SEC eluate fractions

Sample	Particle concentration (p/mL)	Z-average (nm)	PDI (-)	Zeta potential (mV)
UF/DF concentrate	$1.10*10^{12} \pm 1.75*10^{11}$	98	0.502	−27 ± 10
Fraction 2	$1.57*10^{11} \pm 3.32*10^{10}$	148	0.262	−31 ± 9
Fraction 3	$2.39*10^{11} \pm 4.30*10^{10}$	131	0.264	−25 ± 11
Fraction 4	$3.08*10^{10} \pm 7.15*10^{9}$	88.4	0.293	−27 ± 16
Fraction 5	$7.54*10^{09} \pm 1.88*10^{9}$	90.9	0.438	−11 ± 73

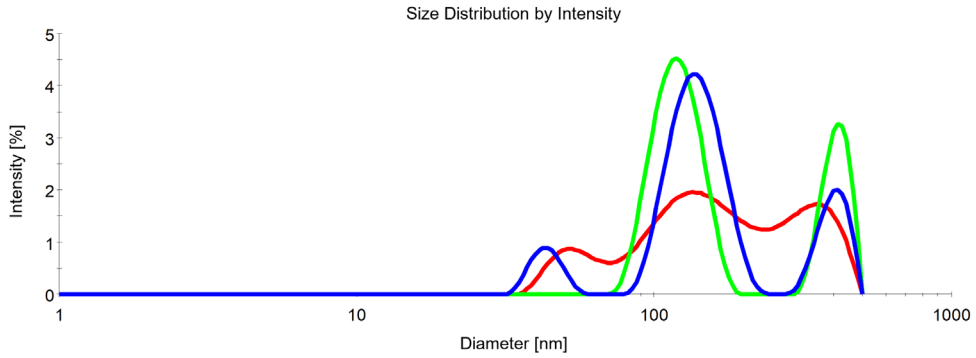

FIGURE 6 Size distribution by intensity of the SEC eluate fraction 3. Analysis was performed in triplicates (red, green and blue lines)

(Table 1), exhibited a high absorbance at 260 and 280 nm (Figure 5) probably due to the nucleic acid and protein load of the EVs [7,8]. This suggests that the measured particles were indeed EVs, which was additionally supported by the size distribution analysis of fraction 3 (Figure 6). Like in the crude UF/DF concentrate sample, the majority of the molecules exhibited a size between 30 and 200 nm (Figures 4A and 6), which is characteristic for EVs. The very low absorbance signal of the first fraction was due to the void volume of the SEC column.

While the validity of the Z-average is limited in EV research due to the high PDI of the samples, the particle sizes decreased with progressing elution from 148 to 90.9 nm while the UF/DF concentrate has a value in between, of 98 nm, which demonstrates how the initial sample is separated via the SEC according to the particle size (Table 1). The rather low value can be explained by the signal of the mAb which was present in the crude sample. In addition, the PDI of fractions 2, 3, and 4 was much lower than that of the UF/DF concentrate, indicating a purer, more uniform sample.

The zeta potential was very similar for fractions 2, 3, and 4 as well as the crude UF/DF concentrate sample as load of the SEC at approximately -30 mV. However, eluate fraction 5 exhibited a less negative zeta potential of -11 mV (Table 1). This was consistent with the low particle concentration, indicating a low amount of EVs in this sample, which are mainly responsible for the negative potential.

The mAb, as impurity model protein in this study, was separated from the EVs by the SEC and eluted between fraction 8 and 14 (Figure 5). This was confirmed by the DLS results, with eluate fraction 3 exhibiting no signal at 10 nm, unlike the crude UF/DF concentrate sample (Figure 4A and 6). The particle absence in the mAb containing fractions also showed, that the used fluorescence based high-resolution flow cytometry did not quantify smaller molecules or impurities like the mAb.

4 | CONCLUDING REMARKS

This study demonstrates the feasibility of an EV enumeration method using fluorescence based high-resolution flow cytometry for commercially available, purified exosome samples as well as crude process samples. This is especially useful for the process development and quality control of biopharmaceutical EVs, where samples of different purities have to be analyzed.

In addition, the size distribution and the zeta potential of the samples were used for further characterization. The samples derived from the CHO cell line exhibited a size between 30 and 200 nm as well as a negative zeta potential of approximately -30 mV, both characteristic values for small EVs.

A SEC was used to successfully separate the EVs from a mAb which was used as a model for impurities in this

study. Only for the fractions at the beginning a high particle concentration was obtained, while later fraction, containing the mAb, did not show any measurable particle concentration.

While further studies need to be performed to characterize the EVs enumerated by the fluorescence based high-resolution flow cytometry, the method offers several benefits compared to state of the art enumeration methods like NTA which are the easy and fast procedure as well as the ability to also measure crude samples.

A selective enumeration of only certain EV subpopulations, such as exosomes, might be possible by the use of fluorescence labeled antibodies against specific surface proteins like the tetraspanins CD9, CD63, or CD81 [43]. By simultaneously staining EV samples with general and specific stains, and multi-channel detection, the EV characterization potential could also be greatly increased. The potential benefits obtainable by the Virus Counter platform together with the proof of concept demonstrated in this study offer great potential to allow a more efficient EV process development.

ACKNOWLEDGMENTS

The authors would like to thank the entire Advanced BioProcessing team of Sartorius corporate research for their support. Special thanks to Michael Olszowy, Michael Minson, and Aslan Dehghani for the fruitful discussions and exchanges.

CONFLICT OF INTEREST

The authors are employees of Sartorius and used some, but not exclusively, products of this company for this study, what might be seen as a potential conflict.

DATA AVAILABILITY STATEMENT

The data that support the findings of this study are available from the corresponding author upon reasonable request.

REFERENCES

1. Colombo M, Raposo G, Théry C. Biogenesis, secretion, and intercellular interactions of exosomes and other extracellular vesicles. Annu Rev Cell Dev Biol. 2014;30:255–289.
2. Willms E, Cabañas C, Mäger I, et al. Extracellular vesicle heterogeneity: subpopulations, isolation techniques, and diverse functions in cancer progression. Front Immunol. 2018;9:738.
3. Raposo G, Stoorvogel W. Extracellular vesicles: exosomes, microvesicles, and friends. J Cell Biol. 2013;200:373–383.
4. Théry C, Witwer KW, Aikawa E, et al. Minimal information for studies of extracellular vesicles 2018 (MISEV2018): a position statement of the International Society for Extracellular Vesicles and update of the MISEV2014 guidelines. J Extracell Vesicles. 2018;7:1535750.
5. Cocucci E, Racchetti G, Meldolesi J. Shedding microvesicles: artefacts no more. Trends Cell Biol. 2009;19:43–51.
6. Cocucci E, Meldolesi J. Ectosomes and exosomes: shedding the confusion between extracellular vesicles. Trends Cell Biol. 2015;25:364–372.
7. Gasser O, Hess C, Miot S, et al. Characterisation and properties of ectosomes released by human polymorphonuclear neutrophils. Exp Cell Res. 2003;285:243–257.
8. Mathivanan S, Ji H, Simpson RJ. Exosomes: extracellular organelles important in intercellular communication. J Proteomics. 2010;73:1907–1920.
9. Corrado C, Raimondo S, Chiesi A, et al. Exosomes as intercellular signaling organelles involved in health and disease: basic science and clinical applications. Int J Mol Sci. 2013;14:5338–5366.
10. Harding CV, Heuser JE, Stahl PD. Exosomes: looking back three decades and into the future. J Cell Biol. 2013;200:367–371.
11. Yoon YJ, Kim OY, Gho YS. Extracellular vesicles as emerging intercellular communicasomes. BMB Rep. 2014;47:531–539.
12. Alvarez-Erviti L, Seow Y, Yin H, et al. Delivery of siRNA to the mouse brain by systemic injection of targeted exosomes. Nat Biotechnol. 2011;29:341–345.
13. Tang K, Zhang Y, Zhang H, et al. Delivery of chemotherapeutic drugs in tumour cell-derived microparticles. Nat Commun. 2012;3:1282.
14. Murphy DE, de Jong OG, Brouwer M, et al. Extracellular vesicle-based therapeutics: natural versus engineered targeting and trafficking. Exp Mol Med. 2019;51:1–12.
15. Gurunathan S, Kang M-H, Jeyaraj M, et al. Review of the isolation, characterization, biological function, and multifarious therapeutic approaches of exosomes. Cells. 2019;8.
16. Wu Y, Deng W, Klinke DJ. Exosomes: improved methods to characterize their morphology, RNA content, and surface protein biomarkers. Analyst. 2015;140:6631–6642.
17. Heath N, Grant L, de Oliveira TM, et al. Rapid isolation and enrichment of extracellular vesicle preparations using anion exchange chromatography. Sci Rep. 2018;8:5730.
18. Lee K, Fraser K, Ghaddar B, et al. Multiplexed profiling of single extracellular vesicles. ACS Nano. 2018;12:494–503.
19. van der Vlist EJ, Nolte-'t Hoen ENM, Stoorvogel W, et al. Fluorescent labeling of nano-sized vesicles released by cells and subsequent quantitative and qualitative analysis by high-resolution flow cytometry. Nat Protoc. 2012;7:1311–1326.
20. Yuana Y, Oosterkamp TH, Bahatyrova S, et al. Atomic force microscopy: a novel approach to the detection of nanosized blood microparticles. J Thromb Haemost. 2010;8:315–323.
21. György B, Módos K, Pállinger E, et al. Detection and isolation of cell-derived microparticles are compromised by protein complexes resulting from shared biophysical parameters. Blood. 2011;117:e39–48.
22. Nolte-'t Hoen ENM, van der Vlist EJ, Aalberts M, et al. Quantitative and qualitative flow cytometric analysis of nanosized cell-derived membrane vesicles. Nanomedicine. 2012;8:712–720.
23. Chuo ST-Y, Chien JC-Y, Lai CP-K. Imaging extracellular vesicles: current and emerging methods. J Biomed Sci. 2018;25:91.
24. Dragovic RA, Gardiner C, Brooks AS, et al. Sizing and phenotyping of cellular vesicles using Nanoparticle Tracking Analysis. Nanomedicine. 2011;7:780–788.

25. Szatanek R, Baj-Krzyworzeka M, Zimoch J, et al. The methods of choice for Extracellular Vesicles (EVs) characterization. Int J Mol Sci. 2017;18.
26. de Necochea-Campion R, Gonda A, Kabagwira J, et al. A practical approach to extracellular vesicle characterization among similar biological samples. Biomed Phys Eng Express. 2018;4:65013.
27. Witwer KW, Buzás EI, Bemis LT, et al. Standardization of sample collection, isolation and analysis methods in extracellular vesicle research. J Extracell Vesicles. 2013;2.
28. Sunkara V, Woo H-K, Cho Y-K. Emerging techniques in the isolation and characterization of extracellular vesicles and their roles in cancer diagnostics and prognostics. Analyst. 2016;141:371–381.
29. Kozak D, Anderson W, Vogel R, et al. Simultaneous size and ζ-potential measurements of individual nanoparticles in dispersion using size-tunable pore sensors. ACS Nano. 2012;6:6990–6997.
30. van der Pol E, Hoekstra AG, Sturk A, et al. Optical and non-optical methods for detection and characterization of microparticles and exosomes. J Thromb Haemost. 2010;8:2596–2607.
31. Perez-Pujol S, Marker PH, Key NS. Platelet microparticles are heterogeneous and highly dependent on the activation mechanism: studies using a new digital flow cytometer. Cytometry A. 2007;71:38–45.
32. Ungureanu C, Rayavarapu RG, Manohar S, van Leeuwen TG. Discrete dipole approximation simulations of gold nanorod optical properties: choice of input parameters and comparison with experiment. J Appl Phys. 2009;105:102032.
33. Dehghani M, Montange RK, Olszowy MW, Pollard D. An emerging fluorescence-based technique for quantification and protein profiling of extracellular vesicles. SLAS Technol. 2021;26:189–199.
34. Kruse T, Kampmann M, Rüddel I, Greller G. An alternative downstream process based on aqueous two-phase extraction for the purification of monoclonal antibodies. Biochem Eng J. 2020;161:107703.
35. Hawe A, Hulse WL, Jiskoot W, Forbes RT. Taylor dispersion analysis compared to dynamic light scattering for the size analysis of therapeutic peptides and proteins and their aggregates. Pharm Res. 2011;28:2302–2310.
36. Midekessa G, Godakumara K, Ord J, et al. Zeta potential of extracellular vesicles: toward understanding the attributes that determine colloidal stability. ACS Omega. 2020;5:16701–16710.
37. Zhang Y, Bi J, Huang J, et al. Exosome: a review of its classification, isolation techniques, storage, diagnostic and targeted therapy applications. Int J Nanomedicine. 2020;15:6917–6934.
38. Busatto S, Vilanilam G, Ticer T, et al. Tangential flow filtration for highly efficient concentration of extracellular vesicles from large volumes of fluid. Cells. 2018;7:273.
39. Han S, Rhee WJ. Inhibition of apoptosis using exosomes in Chinese hamster ovary cell culture. Biotechnol Bioeng. 2018;115:1331–1339.
40. Reth M. Matching cellular dimensions with molecular sizes. Nat Immunol. 2013;14:765–767.
41. Tan YH, Liu M, Nolting B, et al. A nanoengineering approach for investigation and regulation of protein immobilization. ACS Nano. 2008;2:2374–2384.
42. Ren J, Li Z, Wong F-S. A new method for the prediction of pore size distribution and MWCO of ultrafiltration membranes. J Membr Sci. 2006;279:558–569.
43. Kowal J, Arras G, Colombo M, et al. Proteomic comparison defines novel markers to characterize heterogeneous populations of extracellular vesicle subtypes. Proc Natl Acad Sci USA. 2016;113:E968–77.

How to cite this article: Kruse T, Schneider S, Reger LN, Kampmann M, Reif O-W. A novel approach for enumeration of extracellular vesicles from crude and purified cell culture samples. Eng Life Sci. 2022;22:334–343.
https://doi.org/10.1002/elsc.202100149